Carbon Monoxide Hydrogenation on the Ru(001) Surface at Low Temperature Using Gas-Phase Atomic Hydrogen: Spectroscopic Evidence for the Carbonyl Insertion Mechanism on a Transition Metal Surface

William J. Mitchell, Jun Xie, Thomas A. Jachimowski, and W. Henry Weinberg*

Contribution from the Department of Chemical Engineering, University of California, Santa Barbara, California 93106

Received October 14, 1994[⊗]

Abstract: Hydrogenation of carbon monoxide on the Ru(001) surface has been investigated using high-resolution electron energy loss spectroscopy and temperature-programmed desorption. Exposing gas-phase atomic hydrogen to a saturated carbon monoxide overlayer at 100 K results in reaction (via Eley-Rideal kinetics) under ultrahigh vacuum conditions. Both η^1- and η^2-formyl are clearly identified as initial reaction products at low atomic exposures. At higher exposures the production of η^2-formaldehyde is observed. Annealing to 180 K decomposes some of the η^1-formyl, leading to adsorbed CO and hydrogen desorption, with the remainder of the η^1-formyl converting to η^2-formyl. Upon annealing to 220 K, the η^2-formaldehyde decomposes to adsorbed CO and hydrogen which desorbs. Further annealing to 250 K leads to complete decomposition of the η^2-formyl, resulting in hydrogen desorption and regeneration of the original CO overlayer. These identifications represent the first spectroscopic observation of a carbonyl insertion channel operating during carbon monoxide hydrogenation on a well-characterized transition metal surface.

I. Introduction

One of the most important objectives of ultrahigh vacuum (UHV) surface science is to provide fundamental insight into the mechanisms of catalytic reactions of industrial and technological significance. Unfortunately, the preponderance of industrially important *synthesis* reactions, Fischer-Tropsch synthesis, for example, involving the hydrogenation of CO to hydrocarbons and oxygenates, are not amenable to detailed spectroscopic study under UHV conditions. They are primarily "high pressure" phenomena which is a direct result of very low reaction probabilities. In other words, the reaction intermediates are either thermodynamically unfavored ($\Delta H_{rxn} > 0$), kinetically unfavored (the activation barrier for the rate-limiting elementary surface reaction is significantly higher than barriers for competing reactions, such as reactant desorption), or both. In the surface science literature, these observations are embodied by the rubric "pressure gap", and it is this pressure gap that hinders the application of UHV surface science studies to industrial catalysis. Consequently, to "bridge" this gap and determine the intermediates of those reactions which occur with prohibitively low conversions under UHV conditions, one must use alternative methods to probe the reaction path from reactants to products. The most common method is to investigate the reverse (decomposition) reactions of the products by first adsorbing them and then tracing the sequence of steps back through various intermediates until the reactants of the forward synthesis reaction are produced. This procedure has been used extensively to identify possible intermediates resulting from CO hydrogenation on many metal surfaces.[1] For example, in the decomposition of methanol and formaldehyde to adsorbed CO and hydrogen, chemisorbed methoxy, formate, and formyl have been identified and postulated to be relevant intermediates in the reverse hydrogenation reaction.

Another method has been applied to those reactions for which it is difficult to obtain significant concentrations of adsorbed reactants under UHV conditions, due, for example, to an activation barrier separating the initial gas-phase state and the final chemisorbed state. By using supersonic molecular beams, the incident gas-phase molecule can be provided with sufficient translational kinetic energy to overcome the barrier to adsorption (simulating the high-energy tail of the Maxwell-Boltzmann distribution of gas kinetic energies at high pressures) and direct chemisorption of the reactant results. This technique has been used to chemisorb CH_4 dissociatively on a number of different transition metal surfaces (as CH_3 and H)[2] as well as H_2 on copper,[3] even though both of these reactions are activated with

[⊗] Abstract published in *Advance ACS Abstracts,* February 1, 1995.

(1) (a) Demuth, J. E.; Ibach, H. *Chem. Phys. Lett.* **1979**, *60*, 395. (b) Sexton, B. A. *Surf. Sci.* **1981**, *102*, 271. (c) Christmann, K.; Demuth, J. E. *J. Chem. Phys.* **1982**, *76*, 6308. (d) Hrbek, J.; dePaola, R. A.; Hoffmann, F. M. *J. Chem. Phys.* **1984**, *81*, 2818. (e) Rogers, J. W.; Hance, R. L.; White, J. M. *Surf. Sci.* **1980**, *100*, 388. (f) Goodman, D. W.; Yates, J. T.; Madey, T. E. *Surf. Sci.* **1980**, *93*, L135. (g) Bhattacharya, A. K.; Chesters, M. A.; Pebble, M. E.; Sheppard, N. *Surf. Sci.* **1988**, *206*, L845. (h) Stuve, E. M.; Madix, R. J.; Sexton, B. A. *Surf. Sci.* **1982**, *119*, 279. (i) Sexton, B. A.; Hughes, A. E.; Avery, N. R. *Surf. Sci.* **1985**, *155*, 366. (j) Fisher, G. B.; Madey, T. E.; Yates, J. T. *J. Vac. Sci. Technol.* **1978**, *15*, 543. (k) Avery, N. R.; *Langmuir* **1985**, *1*, 162. (l) Richter, L. J.; Ho, W. *J. Chem. Phys.* **1985**, *83*, 2165. (m) Attard, G. A.; Ebert, H. D.; Parsons, R. *Surf. Sci.* **1990**, *240*, 125. (n) Leibsle, F. M.; Francis, S. M.; Davis, R.; Xiang, N.; Haq, S.; Bowker, M. *Phys. Rev. Lett.* **1994**, *72*, 2569. (o) Anton, A. B.; Parmeter, J. E.; Weinberg, W. H. *J. Am. Chem. Soc.* **1985** *107*, 5558. (p) Anton, A. B.; Parmeter, J. E.; Weinberg, W. H. *J. Am. Chem. Soc.* **1986**, *108*, 1823. (q) Avery, N. R.; Weinberg, W. H.; Anton, A. B.; Toby, B. H. *Phys. Rev. Lett.* **1983**, *51*, 682. (r) Anton, A. B.; Avery, N. R.; Toby, B. H.; Weinberg, W. H. *J. Am. Chem. Soc.* **1986**, *108*, 684. (s) Henderson, M. A.; Zhou, Y.; White, J. M. *J. Am. Chem. Soc.* **1989**, *111*, 1185. (t) Delbecq, F.; Sautet, P. *Langmuir* **1993**, *9*, 197. (u) Davis, J. L.; Barteau, M. A. *Surf. Sci.* **1990**, *235*, 235. (v) Houtman, C. J.; Barteau, M. A. *J. Catal.* **1991**, *130*, 528. (w) Brown, N. F.; Barteau, M. A. *Langmuir* **1992**, *8*, 862.

(2) (a) Stewart, C. N.; Ehrlich, G. *J. Chem. Phys.* **1975**, *62*, 4672. (b) Rettner, C. T.; Pfnür, H. E.; Auerbach, D. J. *J. Chem. Phys.* **1986**, *84*, 4163. (c) Verhoef, R. W.; Kelly, D.; Mullins, C. B.; Weinberg, W. H. *Surf. Sci.* **1994**, ***287/288***, 94.

(3) (a) Anger, G.; Winkler, A.; Rendulic, K. D. *Surf. Sci.* **1989**, *220*, 1. (b) Michelson, H. A.; Auerbach, D. J. *J. Chem. Phys.* **94**, 7502 (1991). (c) Winkler, A.; Rendulic, K. D. *Int. Rev. Phys. Chem.* **1992**, *11*, 101.

0002-7863/95/1517-2606$09.00/0

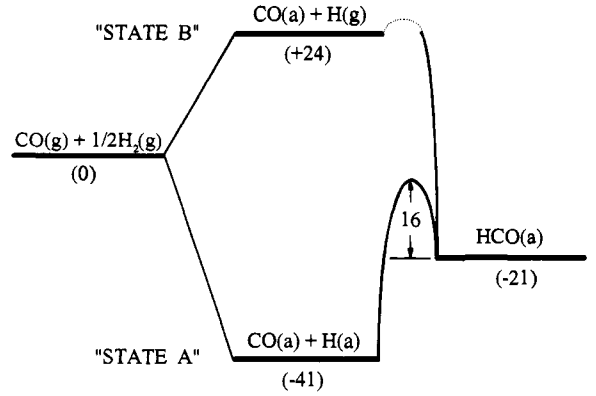

Figure 1. Comparison of the LH and ER mechanisms for CO hydrogenation via carbonyl insertion on the Ru(001) surface. All energies are in kcal/mol.

respect to the gas phase and are, therefore, kinetically unfavorable with respect to unimolecular desorption.

One other emerging technique that has been used to bypass thermodynamic and kinetic limitations which occur during catalytic hydrogenation reactions utilizes a source of gas-phase atomic hydrogen to effect reaction via an Eley–Rideal (ER) mechanism.[4] This method realizes that the limitation to hydrogenation reactions via Langmuir–Hinshelwood (LH) kinetics[5] on many transition metal surfaces is the high strength of the metal–H bond coupled with the low barrier to hydrogen desorption, e.g., approximately 65 and 13 kcal/(mol H), respectively, on Ru(001) at low coverages.[6] By producing the required hydrogen atom for reaction in the gas phase, and not by dissociative chemisorption, the Ru–H bond does not form and, hence, does not need to be activated for reaction to occur. Consider the energy diagram of Figure 1 for CO hydrogenation via a "carbonyl insertion" mechanism, which shows typical values for the Ru(001) surface at low coverages of the Ru–CO (28 kcal/mol)[7] and Ru–H (65 kcal/mol, *vide supra*) bond energies as well as the activation energy for the dissociation of adsorbed HCO (16 kcal/mol, *vide infra*). Since the value of the Ru–HCO binding energy is not known, we first estimate it using the Ni–HCO binding energy (56 kcal/mol) determined theoretically by Goddard and co-workers[8] and then relate it to the zero reference energy by using the heat of formation of gas-phase HCO (+9 kcal/mol).[9] The reaction between coadsorbed H and CO (state A in Figure 1) to form adsorbed HCO is neither kinetically favored (i.e., both hydrogen and CO desorption with activation energies of 13 and 28 kcal/mol, respectively, are preferred to the surface hydrogenation reaction with an activation energy of 36 kcal/mol) nor thermodynamically favored (ΔH_{rxn} of +20 kcal/mol). Thus, the conversion to adsorbed HCO, via LH kinetics, is extremely low. However, if gas-phase atomic hydrogen were used instead (state B in Figure 1), there are no kinetic limitations to adsorbed HCO formation since the incident energy of the H atom exceeds any small barrier which might be associated with the ER reaction. Moreover, this reaction is thermodynamically favored by 45 kcal/mol.

It is therefore plausible that by removing the M–H bond energy from the reaction energetics, we might expect to simulate Fischer–Tropsch chemistry (at least the initiation step) under UHV conditions. Others have used atomic hydrogen as a reactant to investigate the hydrogenation of oxygen adatoms and chemisorbed formate on Ru(001),[10] C:H films on Pt(111),[11] polycrystalline β-SiC,[12] adsorbed ethylene, benzene, and cyclohexane on Cu(111),[13] chlorine adatoms on Au(111),[14] surface methyl groups on Si(100),[15] and deuterium adatoms on Cu(111),[16] polycrystalline diamond,[17] Cu(110),[18] and Ru(001).[19] Most of these reactions do not usually occur under UHV conditions without employing atomic hydrogen.

Developed initially in 1925, the Fischer–Tropsch (FT) synthesis involves the conversion of CO and H_2 under high pressure (order of one to hundreds of atmospheres) over a metallic catalyst (mainly Fe, Co, or Ru) to produce, via oligomerization, linear chain hydrocarbon fuels (favored by lower pressures) and oxygenated chemicals (favored at higher pressures). Despite intensive research efforts during the past 70 years, a complete understanding of the mechanism of this reaction and, in particular, its initiation step still remains unclear. Two mechanistic channels have been proposed, however. The first was suggested originally by Fischer and Tropsch in 1926,[20] and later refined by Craxford and Rideal,[21] who argue that the reaction proceeds via the dissociation of CO to form surface carbides (initiation step) which are then hydrogenated to give adsorbed methylenes. These CH_2 groups oligomerize to form linear-chain hydrocarbons of varying length (chain growth), depending on the catalyst and reactor conditions. This channel is known as the "carbide" mechanism. The other channel, termed the "carbonyl insertion" mechanism, was first proposed in 1958[22] and was later modified[23] based on individual steps which are well established in the organometallic literature, e.g., oxidative addition, reductive elimination, and migratory insertion reactions. This channel proceeds by the insertion of adsorbed CO into either a metal–H bond to form a formyl intermediate (initiation), or a metal–alkyl bond (chain growth) to produce chemisorbed acyls, dehydration of which then results in longer chain alkyls. This mechanism has ample precedent in homogeneous catalysis since several transition metal formyl and

(4) The ER mechanism describes a reaction between a reactant which has chemisorbed and one which has not, i.e., the incident reactant may (indirect) or may not (direct) have dynamically trapped at the surface, but it has not accommodated to the surface temperature.

(5) (a) The majority of surface reactions exhibit LH kinetics,[5b] where the reactants have chemisorbed prior to reaction, i.e., they have both trapped and accommodated to the surface temperature. (b) Weinberg, W. H. In *Dynamics of Gas-Surface Collision*; Rettner C. T., Ashfold, M. N. R., Eds.; Royal Society of Chemistry: Cambridge, 1991.

(6) Feulner, P.; Menzel, D. *Surf. Sci.* **1985**, *154*, 465.

(7) Fuggle, J. C.; Umbach, E.; Feulner, P.; Menzel, D. *Surf. Sci.* **1977**, *64*, 69.

(8) Goddard, W. A.; Walch, S. P.; Rappé, A. K.; Upton, T. H.; Melius, C. F. *J. Vac. Sci. Technol.* **1977**, *14*, 416.

(9) *CRC Handbook of Chemistry and Physics, 70th* ed.; CRC Press: Boca Raton FL, 1990; p F210.

(10) (a) Xie, J.; Mitchell, W. J.; Lyons, K. J.; Wang, Y.; Weinberg, W. H. *J. Vac. Sci. Technol. A* **1994**, *12*, 2210. (b) Xie, J.; Mitchell, W. J.; Lyons, K. J.; Weinberg, W. H. *J. Chem. Phys.* **1994**, *101*, 9195.

(11) Biener, J.; Schubert, U. A.; Schenk, A.; Winter, B.; Lutterloh, C.; Küppers, J. *J. Chem.Phys.* **1993**, *99*, 3125.

(12) Kim, Y.; Olander, D. R. *Surf. Sci.* **1994**, *313*, 399.

(13) (a) Xi, M.; Bent, B. E. *J. Vac. Sci. Technol. A* **1992**, *10*, 2440. (b) Xi, M.; Bent, B. E. *J. Phys. Chem.* **1993**, *97*, 4167.

(14) (a) Lykke, K. R.; Kay, B. D. In *Laser Photoionization and Desorption Surface Analysis Techniques*; Nogar, N. S., Ed.; SPIE, Bellingham WA, 1990; Vol. 1208, p 18. (b) Jackson, B.; Persson, M.; Kay, B. D. *J. Chem. Phys.* **1994**, *100*, 7687. (c) Rettner, C. T. *J. Chem. Phys.* **1994**, *101*, 1529.

(15) Cheng, C. C.; Lucas, S. R.; Gutleben, H.; Choyke, W. J.; Yates, J. T. *Surf. Sci.* **1992**, *273*, L441.

(16) Rettner, C. T. *Phys. Rev. Lett.* **1992**, 69, 383.

(17) Koleske, D. D.; Gates, S. M.; Thoms, B. D.; Russell, J. N.; Butler, J. E. *J. Chem. Phys.*, submitted.

(18) Bischler, U.; Sandl, P.; Bertel, E.; Brunner, T.; Brenig, W. *Phys. Rev. Lett.* **1993**, *70*, 3603.

(19) Jachimowski, T. A.; Weinberg, W. H. *J. Chem. Phys.* **1994**, *101*, 10997.

(20) (a) Fischer, F.; Tropsch, H. *Brenstoff-Chem.* **1926**, *7*, 197. (b) Fischer, F.; Tropsch, H. *Chem. Ber.* **1926**, *59*, 830.

(21) Craxford, S. R.; Rideal, E. K.; *Trans. Faraday Soc.* **1946**, *42*, 576.

(22) Wender, I.; Friedman, S.; Steiner, W. A.; Anderson, R. B. *Chem. Ind.* **1958**, 1694.

(23) (a) Pichler, H.; Schulz, H. *Chem. Ing. Tech.* **1970**, *42*, 1162. (b) Henrici-Olive, G.; Olive, S.; *Angew. Chem. Int. Ed. Engl.* **1976**, *15*, 136.

formaldehyde complexes have been isolated, usually via indirect methods that involve intermolecular hydrogen transfer from borohydrides, BL_3H^- (L = ligand), to cationic metal carbonyls, $M(CO)_n^+$.

Many experimental studies (on both supported and single-crystalline transition metal catalysts) have been performed to identify which of the two channels would be preferred on a particular catalyst. A large group of researchers support the predominance of the carbide channel during FT synthesis.[24] The studies which have been cited as providing the most convincing support for this dominance (e.g., refs. 24h and 24q) are those from the research groups of Biloen and Pettit. Biloen et al.[24m,n] performed isotopic labeling experiments on supported Ni, Co, and Ru catalysts and concluded that the production of hydrocarbons originates primarily from the hydrogenation of surface carbides. Brady and Pettit[24o,p] decomposed diazomethane (CH_2N_2) on various transition metals at atmospheric pressure in order to probe the importance, as suggested by the carbide theory, of methylene intermediates in FT synthesis. They concluded that *only* the carbide mechanism was consistent with their experimental results.

However, it has been argued that these studies do not contradict the reaction behavior expected if the carbonyl insertion mechanism is dominant.[25] In particular, the conclusions of Biloen, et al.[24m,n] were criticized because they are based on only a small percentage of the overall FT products: 22% and 4% of the total product yield in the case of Co and Ru, respectively. Furthermore, studies performed by Emmett, et al.,[26] using the same isotopic labeling techniques as Biloen et al.,[24m,n] found that on Fe and Co catalysts (both of which have the ability to dissociate CO at low pressures) the carbide mechanism could account for no more than 20% of the total Fischer–Tropsch products. Moreover, experimental evidence obtained from the methanation reaction on transition metals (i.e., "lower pressure" FT synthesis where mainly CH_4 is produced) supports this emerging belief that the carbide mechanism is not the only route to FT products. For example, using pulsed reactor and isotopic labeling techniques, it was found that although on Ni surfaces[27] the rate of CH_4 production from surface carbide is an order of magnitude higher than that from adsorbed CO, on Co[27] the two rates are comparable; and on Ru[27a] and Pd[27b] the carbide rate is significantly slower than that from adsorbed CO. Furthermore, *ex situ* spectroscopic analysis (Auger and X-ray photoelectron spectroscopies), performed on single-crystalline Fe, Ni, and Ru crystals[28] after reaction at 10–1000 Torr, reveals that a decrease in the CH_4 production rate is correlated with an increase in the surface carbon concentration, Θ_C. In all cases this result was interpreted in terms of the carbide mechanism only. On Fe it was claimed that the formation of inert graphitic islands at higher Θ_C reduces the surface concentration of active carbide which, in turn, lowers the carbide hydrogenation rate. On Ni and Ru the higher Θ_C was claimed to inhibit hydrogen adsorption which results in lower carbide hydrogenation rates. This behavior, however, can also be interpreted in terms of carbonyl insertion where the surface carbide/graphite serves to block CO adsorption and, hence, lowers the rate of its hydrogenation.

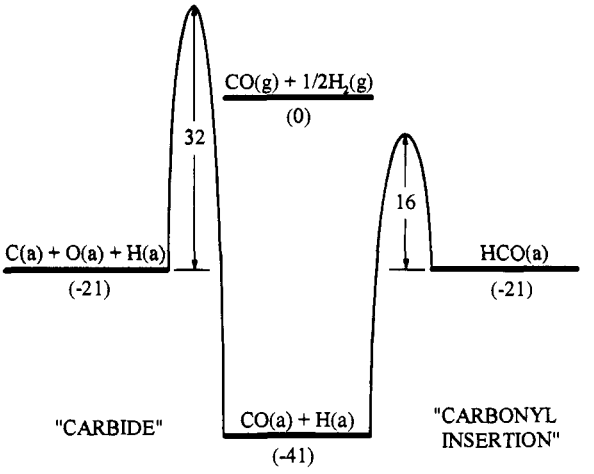

Figure 2. Comparison of the carbide and carbonyl insertion channels (via LH kinetics) for CO hydrogenation on the Ru(001) surface. All energies are in kcal/mol.

Consequently, it is not clear that one can assert the predominance of either the carbide mechanism or the carbonyl insertion mechanism on any particular FT catalyst during FT synthesis. On Ru(001) it is possible to compare the energetics of the competing initiation steps for each channel, as shown in Figure 2. The data presented in Figure 1 are used for the carbonyl insertion channel, and for the carbide channel an estimate of the Ru–C bond energy (approximately 165 kcal/mol) is taken from Bell.[24q] The activation energy at low carbon coverages for the surface C + O recombination reaction (to produce gas-phase CO) is estimated from carbon titration experiments performed in our laboratory. The overall thermodynamics of the two reactions are essentially identical, both being unfavored by 20 kcal/mol.[29] Moreover, neither initiation step is favored kinetically with respect to reactant desorption, since CO and hydrogen desorb, rather than react, in both the carbide and insertion channels (reaction activation energies of 52 and 36 kcal/mol, respectively). Consistent with this analysis, no chemical reaction between coadsorbed CO and hydrogen on any transition metal surface has been observed under UHV conditions.[30] More importantly, however, is the expectation that the

(24) (a) Low, G.; Bell, A. T. *J. Catal.* **1979**, *57*, 397. (b) Kellner, C. S.; Bell, A. T. *J. Catal.* **1981**, *70*, 418. (c) Eckerdt, J. G.; Bell, A. T. *J. Catal.* **1979**, *58*, 170. (d) Wang, C. J.; Eckerdt, J. G. *J. Catal.* **1984**, *86*, 239. (e) Matsumoto, H.; Bennett, C. O. *J. Catal.* **1978**, *53*, 331. (f) Reymond, J. P.; Merideau, P; Pommier, B; Bennett, C. O. *J. Catal.* **1980**, *64*, 163. (g) Goodman, D. W. *Acc. Chem. Res.* **1984**, *17*, 194. (h) Zheng, C.; Apeloig, Y.; Hoffmann, R. *J. Am. Chem. Soc.* **1988**, *110*, 749. (i) Falbe, J.; Frohning, C. D. *J. Mol. Catal.* **1982**, *17*, 117. (j) Nijs, N. H.; Jacobs, P. A. *J. Catal.* **1980**, *66*, 401 (l) Rofer-de-Poorter, C. *Chem. Rev.* **1981**, *81*, 447. (m) Biloen, P.; Helle, J. N.; Sachtler, W. M. H. *J. Catal.* **1979**, *58*, 95. (n) Biloen, P.; Helle, J. N.; van den Berg, F. G. A.; Sachtler, W. M. H. *J. Catal.* **1983**, *81*, 450. (o) Brady, R. C.; Pettit, R. *J. Am. Chem. Soc.* **1980**, *102*, 6181. (p) Brady, R. C.; Pettit, R. *J. Am. Chem. Soc.* **1981**, *103*, 287. (q) Bell, A. T. *Catal. Rev. Sci. Eng.* **1981**, *23*, 203.

(25) (a) Henrici-Olive, G.; Olive, S. *J. Mol. Catal.* **1982**, *16*, 111. (b) Henrici-Olive, G.; Olive, S. *J. Mol. Catal.* **1983**, *18*, 367. (c) Pichler, H. *Advan. Catal.* **1952**, *4*, 271.

(26) (a) Kummer, J. T.; DeWitt, T. W.; Emmett, P. H. *J. Am. Chem. Soc.* **1948**, *70*, 2632. (b) Kummer, J. T.; Browning, L. C.; Emmett, P. H. *J. Chem. Phys.* **1948**, *16*, 739. (c) Browning, L. C.; DeWitt, T. W.; Emmett, P. H. *J. Am. Chem. Soc.* **1950**, *72*, 4211.

(27) (a) Sachtler, J. W. A.; Kool, J. M.; Ponec, V. *J. Catal.* **1979**, *56*, 284. (b) Rabo, J. A.; Risch, A. P.; Poutsma, M. L. *J. Catal.* **1978** *53*, 295.

(28) (a) Bonzel, H. P.; Krebs, H. J. *Surf. Sci.* **1982**, *117*, 639. (b) Kelley, R. D.; Goodman, D. W. *Surf. Sci.* **1982**, *123*, L743.

(29) This thermodynamic limitation can be reduced somewhat by the action of competing reactions that affect the dynamic equilibrium between the reactants and products of the initiation step. For example, in the carbide channel, surface oxygen can be depleted by hydrogenation or by CO disproportionation to produce H_2O and CO_2, respectively, whereas in the carbonyl insertion channel, further hydrogenation of the adsorbed formyl to formaldehyde and hydroxymethyl can occur.

(30) (a) Peebles, D. E.; Schreifels, J. A.; White, J. M. *Surf. Sci.* **1982**, *111*, 117. (b) Nyberg, G.; Westerlund, L. *Surf. Sci.* **1991**, *256*, 9. (c) Ibbotson, D. E.; Wittrig, T. S.; Weinberg, W. H. *Surf. Sci.* **1981**, *111*, 149. (d) Chesters, N. D. S.; Chesters, M. A. *Surf. Sci.* **1986**, *175*, L811. (e) Benziger, J.; Madix, R. *Surf. Sci.* **1978**, *77*, L379. (f) Conrad, H.; Ertl, G.; Latta, E. E. *J. Catal.* **1974**, *35*, 363. (g) Goodman, D. W.; Yates, J. T.; Madey, T. E.*Surf. Sci.* **1980**, *93*, L315. (h) Gland, J. L.; Fischer, D. A.; Parker, D. H.; Shen, S. *Langmuir* **1991**, *7*, 2574.

carbide and carbonyl insertion channels might *both* contribute significantly to the overall FT synthesis rate (via LH kinetics) on Ru catalysts.

In this report, we continue our work[31] on identifying, via temperature-programmed desorption (TPD) and high-resolution electron energy loss spectroscopy (HREELS), the reaction products (namely, adsorbed formyls and formaldehyde) that result when a saturated CO overlayer on the Ru(001) surface is exposed to gas-phase atomic hydrogen under UHV conditions. This work lends support to the presence of the carbonyl insertion channel during the catalytic hydrogenation of CO on Ru, since one of this mechanism's major shortcomings previously was the inability to synthesize and isolate, under any conditions, the proposed reaction intermediates on a transition metal surface.

II. Experimental Methods

Details of the HREEL spectrometer and the UHV chamber in which it is contained have already been given.[32] The resolution of the spectrometer varied between 30 and 55 cm^{-1} (full-width at half-maximum), while maintaining a count rate of at least 10^5 Hz in the elastically scattered beam in the specular direction. Incident beam energies of approximately 5.5 eV were employed.

The TPD experiments were performed in a separate UHV chamber that has been described in detail elsewhere.[33] In particular, this TPD chamber is equipped with a differentially pumped mass spectrometer (UTI 100C) which is housed inside an (inert) stainless steel cone which prevents mass collection from spurious sources such as the crystal supports and heating leads. This configuration of the mass spectrometer, which cannot be installed in the HREELS chamber due to EEL spectrometer restrictions, proves to be especially important when collecting hydrogen TPD spectra after using the hot filament radical beam doser. Due to the lack of directionality of this source and the activity of the atomic hydrogen which is generated, adsorption occurs not only on the Ru(001) crystal but also on all other parts of the cryostat as well, e.g., the copper crystal supports and clamps. This leads to significant hydrogen degassing when heating the crystal. TPD spectral collection and control were performed with an IBM-compatible PC. All TPD data were measured at a constant heating rate of 5 K/s.

In the HREELS chamber, the Ru(001)-oriented single crystal was mounted on a home-built radiation-shielded cryostat[34] which can cool the crystal to 78 K with liquid nitrogen cooling and below 25 K with liquid helium cooling (not used in the present study). In the TPD chamber, the lowest possible crystal temperature is 90 K with liquid nitrogen cooling. Crystal temperatures were monitored using a type-C thermocouple spotwelded to the back of the crystal. The Ru samples were cleaned using standard techniques of Ar^+ sputtering as well as annealing in oxygen and *in vacuo* to 1650 K to remove chemisorbed oxygen. Surface cleanliness was monitored with HREELS, where a clean surface results in a featureless spectrum, as well as with CO TPD spectra.

Both H and D atoms were generated *in situ* by dissociating H_2 (Matheson, 99.9995%) and D_2 (Matheson, 99.5%) with a hot tungsten filament (approximately 1800 K, as measured by a pyrometer) positioned 1 in. from the crystal. All gases were used without further purification, and their mass spectra gave no indication of impurities. The tungsten filament is housed inside an air-cooled copper radiation shield which is mounted on the end of a $^1/_4$ in. diameter tube through which the H_2 (or D_2) gas is passed. The other end of the tube is connected to a leak valve. During exposure to the atomized hydrogen, the surface temperature increases by approximately 20 and 30−50 K in the HREELS and TPD chambers, respectively, due to radiation from the hot filament.

The atomic hydrogen exposures are reported in Langmuirs (1 L ≡ 10^{-6} Torr-s) and are estimated from the background molecular hydrogen pressure by assuming an atomic flux that is 5% of the molecular flux, a value which has been estimated from hydrogen abstraction TPD data measured previously in the TPD chamber.[19]

The saturated CO overlayer on the Ru(001) surface (Θ_{CO} = 0.65) was prepared by backfilling the UHV chamber through a leak valve and exposing 6 L CO (Matheson, 99.99%) to the surface at 78 K and then annealing to 270 K to order the overlayer. Loss features at 445 and 2060 cm^{-1} in the HREEL spectrum[35] and well-separated desorption peaks at 370 and 450 K in the TPD spectrum[36] are characteristic of the saturated overlayer with CO occupying on-top sites.

III. Experimental Results

A. Temperature-Programmed Desorption Mass Spectrometry. Before discussing our TPD results, we review briefly the TPD data obtained from the coadsorption of hydrogen and CO on Ru(001). A result of particular significance is that molecular hydrogen does not adsorb on the CO-saturated Ru(001) surface.[30a] Adsorption of CO on the hydrogen-saturated Ru(001) surface (Θ_H = 1) results in a CO fractional coverage of 0.15.[30a] Hydrogen desorbs in a single peak with a maximum at 307 K which is downshifted from 322 K in the the absence of CO.[37]

The TPD mass spectra were recorded for varying post-exposures of atomic hydrogen on saturated CO overlayers on Ru(001) at surface temperatures between 110 and 130 K (depending on exposure time in front of the hot filament). In all cases, *only* hydrogen and CO were observed to desorb from the surface, and the desorption spectra of CO are identical to those from the clean surface (since surface hydrogen, in whatever form, has desorbed by 300 K).

The TPD spectra measured after atomic deuterium exposures of 5, 20, and 45 L are shown in Figure 3.[38] Figure 3a shows that for exposures of 5 L of atomic deuterium, D_2 desorption is observed (with two peaks) from a surface that does not adsorb molecular hydrogen (*vide supra*). The low-temperature peak has a maximum at 200 K and is broadened by a low-temperature shoulder and the sharper high-temperature peak is centered at 260 K. After higher exposures (i.e., 20 L and greater), the high-temperature peak shifts slightly upward in temperature to 280 K while maintaining its intensity, and the low-temperature peak at 200 K increases in intensity.[39] A surprising result, however, is the appearance of a peak in the spectra at 240 K after these higher exposures. This behavior cannot be easily explained by

(31) (a) Mitchell, W. J.; Wang, Y.; Xie, J.; Weinberg, W. H.; *J. Am. Chem. Soc.* **1993**, *115*, 4381. (b) Mitchell, W. J.; Xie, J.; Wang, Y.; Weinberg, W. H. *J. Electron Spectrosc. Relat. Phenom.* **1993**, *64/65*, 427.

(32) (a) Thomas, G. E.; Weinberg, W. H. *Rev. Sci. Instrum.* **1979**, *50*, 497. (b) Anton, A. B.; Ph.D. Thesis, California Institute of Technology, 1985. (c) Xie, J.; Mitchell, W. J.; Wang, Y.; Schick, M.; Weinberg, W. H. *Rev. Sci. Instrum.*, submitted for publication.

(33) Taylor, J. L.; Ibbotson, D. E.; Weinberg, W. H. *J. Chem. Phys.* **1978**, *69*, 4298.

(34) Mitchell, W. J.; Wang, Y.; Xie, J.; Weinberg, W. H., manuscript in preparation.

(35) (a) Thomas, G. E.; Weinberg, W. H. *J. Chem. Phys.* **1979**, *70*, 1437. (b) Pfnür, H.; Menzel, D.; Hoffmann, F. M.; Ortega, A.; Bradshaw, A. M. *Surf. Sci.* **1980**, *93*, 431.

(36) Pfnür, H.; Menzel, D. *J. Chem. Phys.* **1983**, *79*, 4613.

(37) Jachimowski, T. A., unpublished results.

(38) Only desorption data obtained with deuterium are presented here. The major features in both hydrogen and deuterium spectra are the same. Any isotopic shift in the desorption peak temperatures is unresolvable.

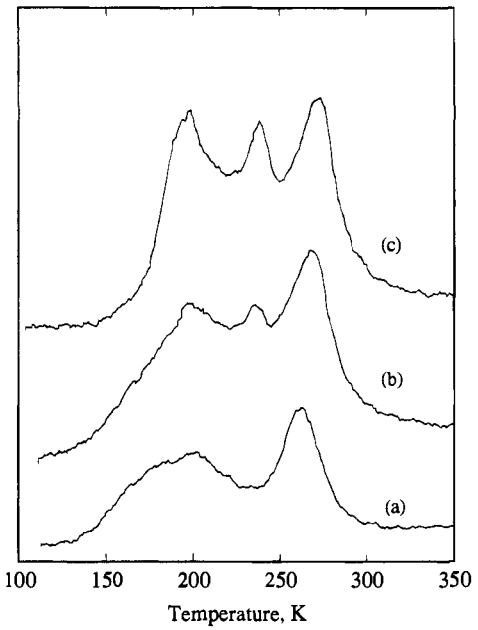

Figure 3. Temperature-programmed desorption spectra showing the evolution of D_2 following approximate atomic deuterium exposures of (a) 5, (b) 20, and (c) 45 L on a saturated overlayer of CO on the Ru-(001) surface at 110−130 K. The heating rate is 5 K/s.

lateral interactions among the coadsorbed hydrogen and CO. A more reasonable explanation involves a chemical reaction which forms a hydrogen-containing intermediate that decomposes near 240 K.

Estimates for the activation energies for each deuterium desorption peak were obtained by applying the method of Redhead[40] and assuming first-order preexponential factors of 10^{13} s^{-1}. The analysis gives approximate activation energies of 11.5, 14.3, and 16.3 kcal/mol for the peaks at 200, 240, and 280 K, respectively.

B. High-Resolution Electron Energy Loss Spectroscopy. Before discussing our EELS results, we will first summarize the EEL spectra measured after adsorbing CO on a saturated hydrogen overlayer on Ru(001).[41] Peaks at 2045 and 1860 cm^{-1} identify CO adsorbed in on-top and bridge sites,[42] respectively. Weak modes at 815 and 1135 cm^{-1} are assigned to the parallel and perpendicular vibrations of the H adatoms.

Shown in Figures 4 and 5 are HREEL spectra measured after exposure of the saturated CO overlayer to 5 L of atomic deuterium and hydrogen, respectively, at a surface temperature of 100 K, followed by annealing to the temperatures indicated in the figure captions. The surface is first heated to 150 K for 60 s, cf., Figures 4a and 5a, to remove some of the water adsorbed from the background (generated by H/D atoms striking the chamber walls). Although annealing to 150 K will not affect the initial intermediates that produce the 200 and 260 K peaks in the D_2 TPD spectrum of Figure 3a, the low-temperature shoulder on the 200 K peak will be severely depleted. A comparison between HREEL spectra recorded at 100 and 150 K, however, shows no noticeable differences (apart from the water features). Therefore, we tentatively assign the low-temperature shoulder in the TPD spectra to the recombinative desorption of hydrogen adatoms since adsorbed hydrogen exhibits only weak vibrational features as a result of a small inelastic electron scattering cross section, i.e., the Ru−H (Ru-D) losses near 800 and 1150 cm^{-1} (500 and 900 cm^{-1}) that should be present at 100 K (and absent at 150 K) are masked by losses from other adsorbed species. Comparison of the spectra at 150 K in Figures 4 and 5 allows immediate identification of the modes at 1735−1740 cm^{-1} as well as 2000−2010 cm^{-1} to carbon−oxygen stretching vibrations since there is no significant isotopic shift. The strong features resolved at 895 and 945 cm^{-1} are assigned to CD bending modes in Figure 4a. These features are estimated to shift to approximately 1140 and 1200 cm^{-1} in the hydrogenated surface species, cf., Figure 5a, by using a typical isotopic shift factor of 1.27 for CD bends.[43] The inversion in relative intensity of these two bending modes in the hydrogenated species, as compared to the intensities in the deuterated species, suggests that there is a peak at about 1200 cm^{-1} in both Figures 4a and 5a that does not shift with the hydrogen isotope, hence, identifying an additional carbon−oxygen stretching vibration. In other words, in the hydrogen spectrum of Figure 5a, the 1200 cm^{-1} feature is a result of overlapping peaks due to a CO stretch and a CH bend. Features at 2200 and 2970 cm^{-1} (much more clearly resolved in off-specular spectra which are not shown) are assigned to carbon−hydrogen stretching vibrations, ν(CD) and ν(CH), respectively. With reference to HREEL spectra obtained for water adsorption on Ru(001),[44] the modes at 2580 and 3460 cm^{-1} in Figures 4a and 5a are assigned to ν(OD) and ν(OH) of residual surface water, respectively. The shoulders at approximately 1250 and 1650 cm^{-1} in these two figures are assigned to the water scissoring modes, $\delta(D_2O)$ and $\delta(H_2O)$, respectively. The small peak at 940 cm^{-1} in Figure 5a is discussed below.

With these assignments in mind, and with particular reference to the three carbonyl bands that were observed, it is possible to identify the initial reaction intermediates that result after lower atomic exposures, i.e., 5 L. The band near 2000 cm^{-1} is due to unreacted CO; the band near 1750 cm^{-1} represents a double bond between carbon and oxygen (i.e., the carbon atom has rehybridized from sp in CO to sp^2) which suggests η^1(C)-HCO;[43,45] the band near 1200 cm^{-1} identifies a carbon−oxygen bond, the order of which has decreased significantly below two, suggesting η^2-coordination and, hence, η^2(C,O)-HCO.[1o,p,46] Justification of these assignments can be obtained by comparison with vibrational data available in the literature, as summarized in Tables 1 and 2.

After annealing to 180 K for 60 s, cf., Figures 4b and 5b, the η^1-formyl has largely decomposed or converted to some other species, as judged by the significant decrease of the band at 1740 cm^{-1} in both spectra. A peak at 1820−1840 cm^{-1} which identifies CO that is chemisorbed in a bridge site (*vide supra*) resulting from decomposition of the η^1-formyl and the presence of coadsorbed hydrogen. Furthermore, the increase in both frequency and intensity of the mode at 2030−2040 cm^{-1} in these spectra (upshifted from 2000−2010 cm^{-1}) is evidence for additional on-top CO. From Figure 4b, we see that there is a

(39) After 45 L atomic exposure, the low-temperature shoulder is significantly reduced as a result of the surface temperature increasing to about 130 K in the TPD chamber during the long (approximately 20 min) exposure time.

(40) Redhead, P. A. *Vacuum* **1962**, *12*, 203.
(41) Mitchell, W. J., unpublished results.
(42) Kostov, K. L.; Rauscher, H.; Menzel, D. *Surf. Sci.* **1992**, *278*, 62.
(43) Shimanouchi, T. *Tables of Molecular Vibrational Frequencies-Consolidated Vol. 1*; NSRDS-NBS No. 39; Washington, DC, 1972.
(44) Thiel, P. A.; Hoffmann, F. H.; Weinberg, W. H. *J. Chem. Phys.* **1981**, *75*, 5556.
(45) (a) Wayland, B. B.; Woods, B. A. *J. Chem. Soc., Chem. Commun.* **1981**, *700*. (b) Floriani, C. *Pure Appl. Chem.* **1983**, *55*, 1. (c) Casey, C. P.; Meszaros, M. W.; Neumann, S. M.; Cesa, I. G.; Haller, K. J. *Organometallics* **1985**, *4*, 143.
(46) (a) Koga, N.; Morokuma, K. *New J. Chem.* **1991**, *15*, 749. (b) Tatsumi, K.; Nakamura, A.; Hofmann, P.; Stauffert, P.; Hoffmann, R. *J. Am. Chem. Soc.* **1985**, *107*, 4440. (c) Rappé, A. K. *J. Am. Chem. Soc.* **1987**, *109*, 5605. (d) Curtis, M. D.; Shiu, K.-B.; Butler, W. M. *J. Am. Chem. Soc.* **1986**, *108*, 1550 .

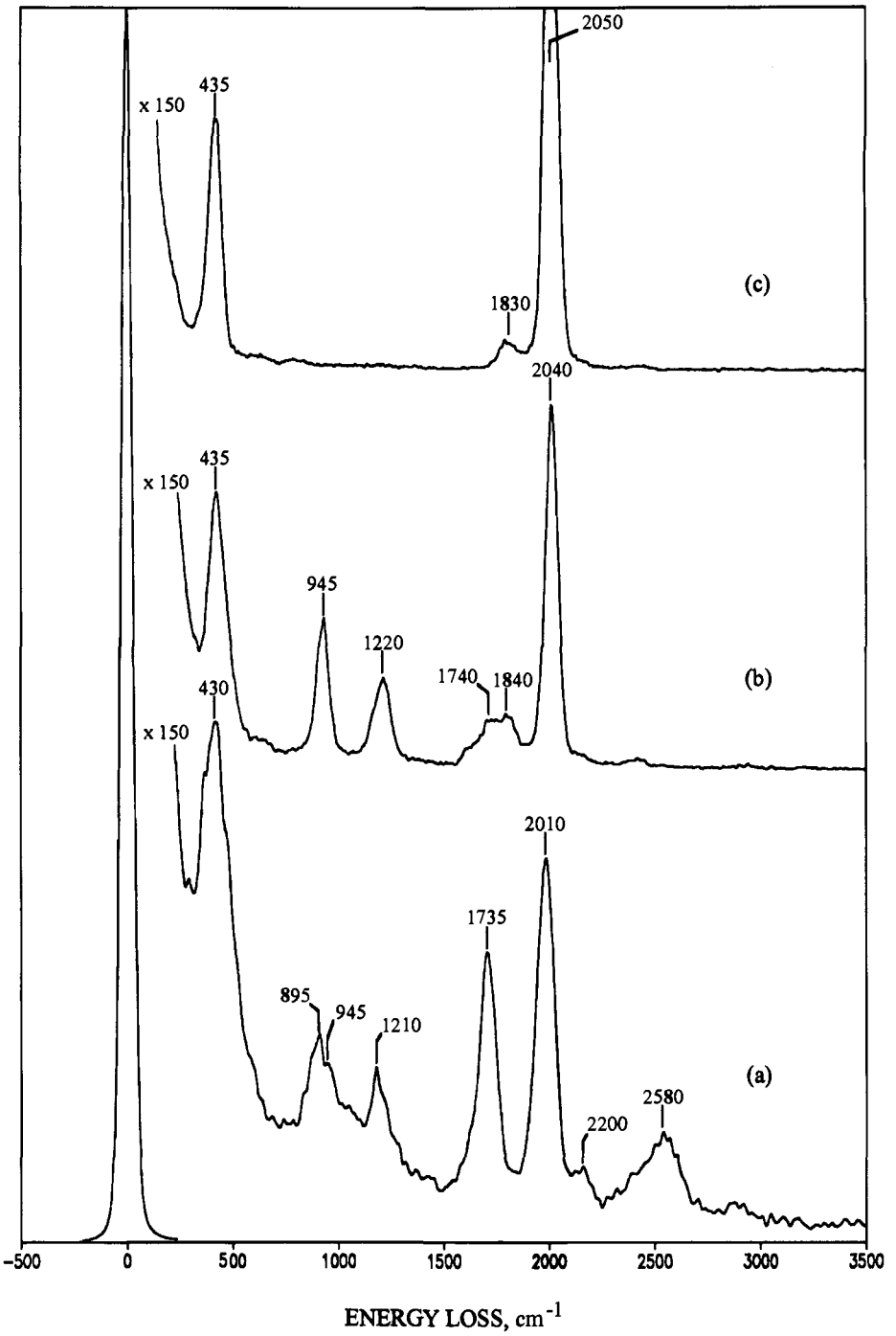

Figure 4. HREEL spectra recorded after exposure of a saturated overlayer of CO on Ru(001) to approximately 5 L of atomic deuterium at 100 K, followed by annealing to (a) 150 K, (b) 180 K, and (c) 250 K.

slight increase in the intensity of the peak of ν(CO) of η^2-DCO (upshifted slightly to 1220 cm^{-1}), and we see in Figures 4b and 5b a clear increase in the intensity of the peak at 940 cm^{-1}, a part of which is due to a CD bending mode in η^2-DCO. The other bending mode of η^2-DCO is not resolved. Since the bending mode at 895 cm^{-1} has attenuated appreciably, cf., Figure 4 (parts a and b), we assign it to η^1-DCO. These assignments are supported by Figure 5b since the peak at 1190 cm^{-1} has increased in intensity (containing the overlapping CH bend and CO stretch of η^2-HCO) and is now very narrow due to a decrease in the CH bend of η^1-HCO at approximately 1140 cm^{-1}.

The peak that appears at 940 cm^{-1} in Figures 5 (parts a and b) cannot be assigned to an increase in the intensity of the other unresolved CH bending mode of η^2-HCO since this peak is not observed to shift down in frequency upon deuteration, i.e., the corresponding bending mode in η^2-DCO is not resolved. This implies that the mode involves mainly CO motion, and we recall that its increase in intensity correlates with the decomposition of η^1-HCO. Therefore, we tentatively assign this peak to a second form of η^2-HCO bound to the surface such that its C−O bond is weakened (bond order of approximately one) compared to the initially formed η^2-HCO (bond order between one and two). An analogy is the weaker CO bond of bridge-bonded CO that is also produced by the decomposition of η^1-HCO. We conclude therefore that the η^1-formyl intermediate is removed by two channels: decomposition to adsorbed CO (bridge and on-top sites) with desorbing hydrogen (the 200 K peak in the hydrogen TPD spectra) as well as conversion to η^2-formyl

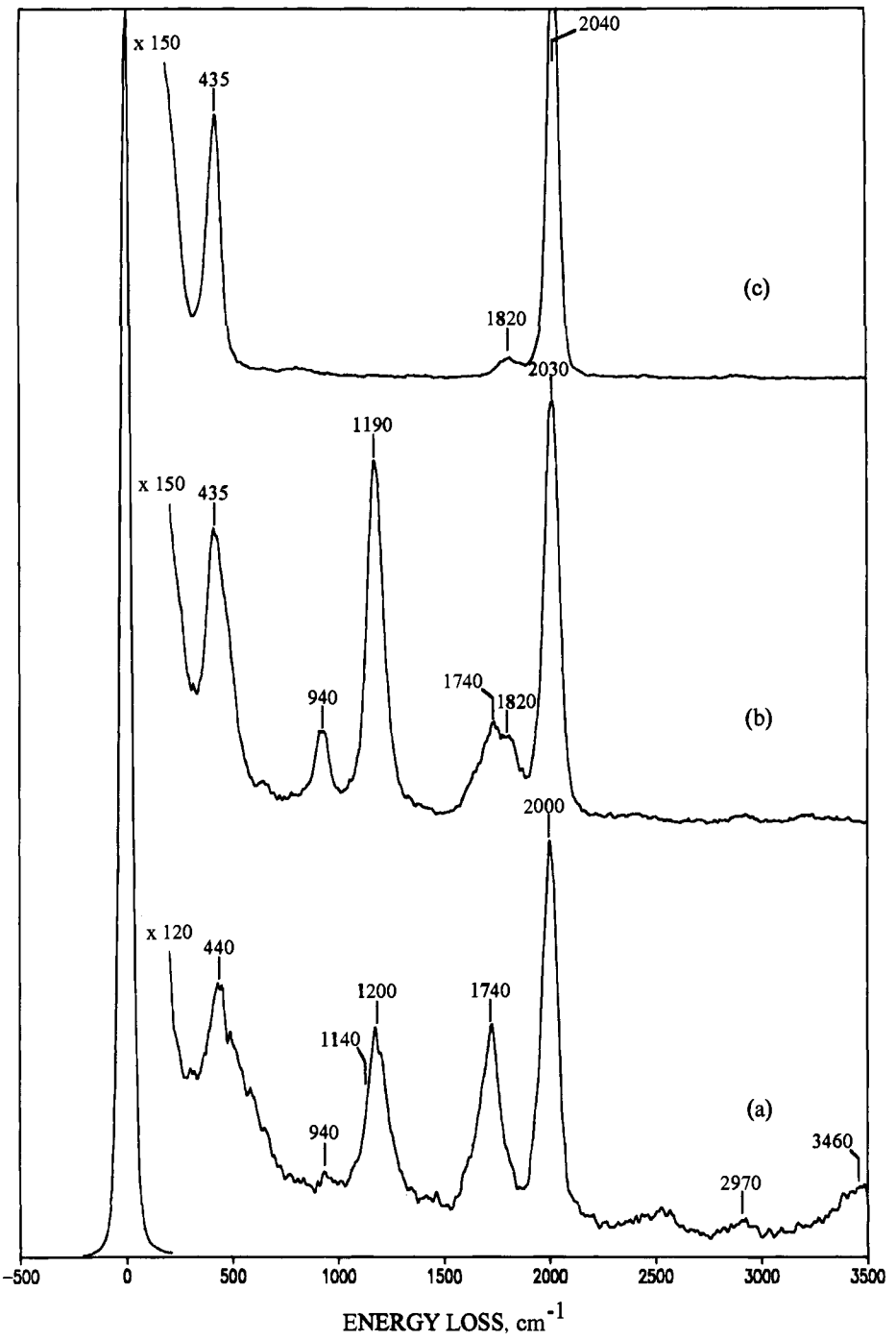

Figure 5. HREEL spectra recorded after exposure of a saturated overlayer of CO on Ru(001) to approximately 5 L of atomic hydrogen at 100 K, followed by annealing to (a) 150 K, (b) 180 K, and (c) 250 K.

(primarily one with an unusually low C−O stretching frequency).

The HREEL spectra measured after annealing the surface at 250 K for 60 s, cf., Figures 4c and 5c, show an increase in frequency and intensity in the peak due to linearly adsorbed CO at 2040−2050 cm^{-1}, whereas those modes characteristic of the η^2-formyls are absent, indicating that they have both decomposed to CO and hydrogen which desorbs (identifying the source of the TPD peak of hydrogen at 270 K).

The HREEL spectra recorded after exposures of 20 L of atomic deuterium and hydrogen on the saturated CO surface at 100 K are shown in Figures 6 and 7. Using the assignments above for the 5 L exposures, we can easily identify the modes due to η^1- and η^2-formyls in the spectra after annealing to 150 K, cf., Figures 6a and 7a. For the η^1-formyl the CO stretch lies at 1710−1720 cm^{-1} and a CD (CH) bend at 900 (approximately 1150) cm^{-1}, whereas for the η^2-formyl, the CO stretch and CH bend overlap at approximately 1220 cm^{-1}. This bending mode is more clearly resolved at 950 cm^{-1} in the deuterated species, cf., Figure 6a. The unreacted CO is identified by the CO stretch at 1960−1970 cm^{-1}, and its intensity has now fallen below that of ν(CO) for the η^1-formyl.

From the TPD spectra of Figure 3, we expect the appearance of new peaks in the HREEL spectra which identify the new surface intermediate responsible for the 240 K TPD peak after 20 L exposure. Although no new peaks can be easily identified after a casual inspection of Figures 6 and 7, a more detailed comparison between the HREEL spectra measured after 5 and 20 L atomic exposures at 150 K reveal subtle differences. For instance, the strong band assigned to the CD bending modes of

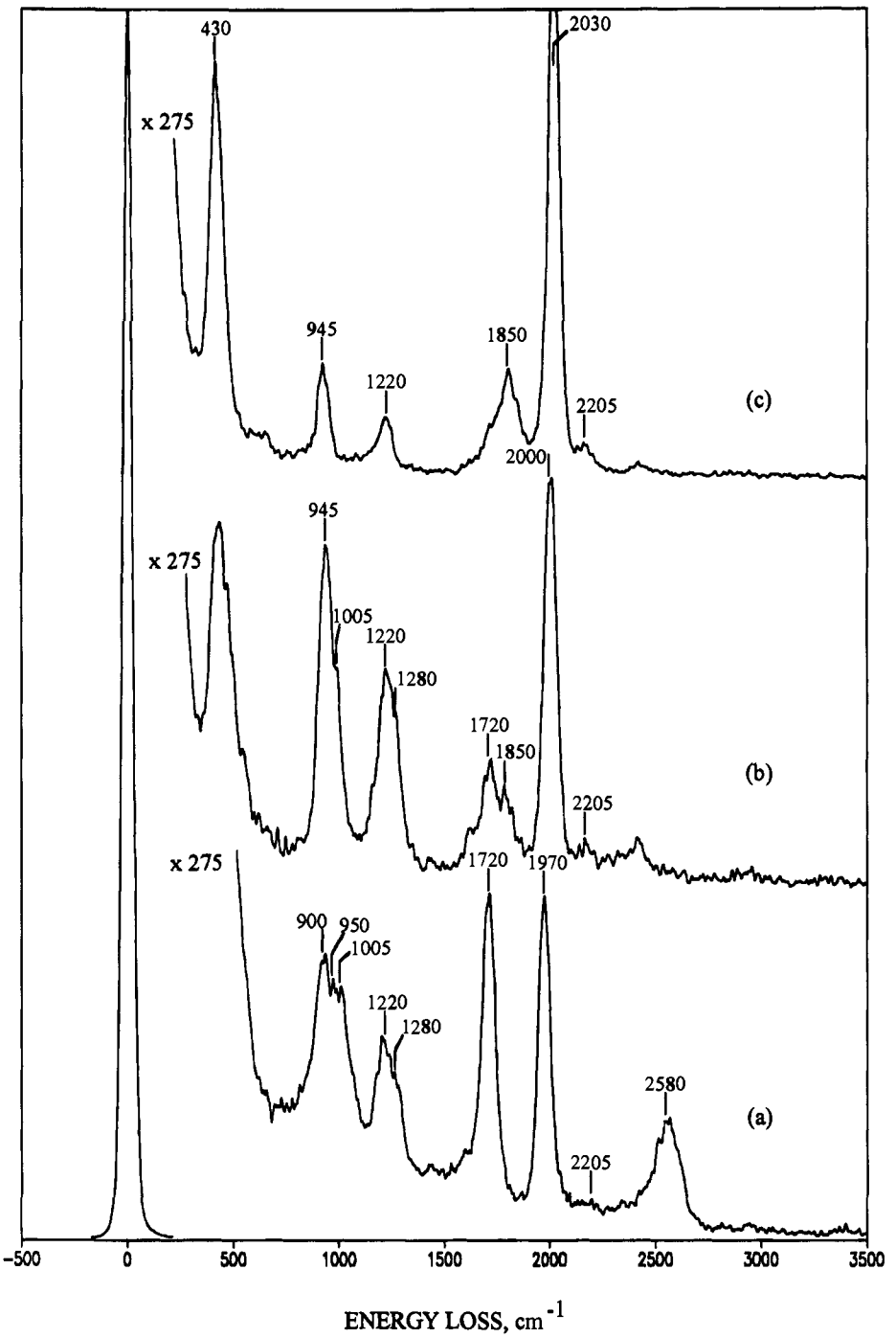

Figure 6. HREEL spectra recorded after exposure of a saturated overlayer of CO on Ru(001) to approximately 20 L of atomic deuterium at 100 K, followed by annealing to (a) 150 K, (b) 180 K, and (c) 220 K.

the η^1- and η^2-formyls at 900−950 cm^{-1} in Figures 4a and 5a includes a strong shoulder at 1005 cm^{-1} after 20 L exposure, cf., Figure 6a. This shoulder shifts to approximately 1280 cm^{-1} in the hydrogenated species, cf., Figure 7a, and is therefore assigned to a carbon−hydrogen mode in the new intermediate. Furthermore, the peak assigned to the CO stretch of η^2-DCO at 1200 cm^{-1} after 5 L of atomic deuterium, cf., Figure 4a, upshifts to 1220 cm^{-1} after 20 L exposures and exhibits a pronounced asymmetry to higher frequencies by virtue of a shoulder at approximately 1280 cm^{-1}, cf., Figure 6a. This shoulder cannot be solely assigned to the $\delta(D_2O)$ mode of surface water. After 20 L of atomic hydrogen, cf., Figure 7a, this band peaks at 1260 cm^{-1} and is now asymmetric to lower frequencies. However, as detailed earlier in the discussion of the 5 L spectra, we can explain this behavior by concluding that the modes at 1220 and 1280 cm^{-1} in the deuterated species are a result of CO stretching vibrations which do not shift significantly after isotopic substitution. Thus, the band centered at 1260 cm^{-1} in the hydrogen spectrum of Figure 7a consists of three separate peaks at approximately 1150 cm^{-1} (CH bend of η^1-HCO), 1220 cm^{-1} (overlapping CH bend and CO stretch of η^2-HCO), and 1280 cm^{-1} (overlapping carbon−hydrogen mode and CO stretch of a new intermediate). The relative intensity and position of the peaks at 1220 and 1280 cm^{-1} are such that their combination gives rise to an apparent maximum which lies between them at 1260 cm^{-1}. The third peak at 1150 cm^{-1} accentuates the asymmetry of the band to lower frequencies.

Summarizing, we find that a new intermediate is produced in detectable quantities (as far as HREELS and TPD are concerned) only after higher atomic exposures, i.e., greater than

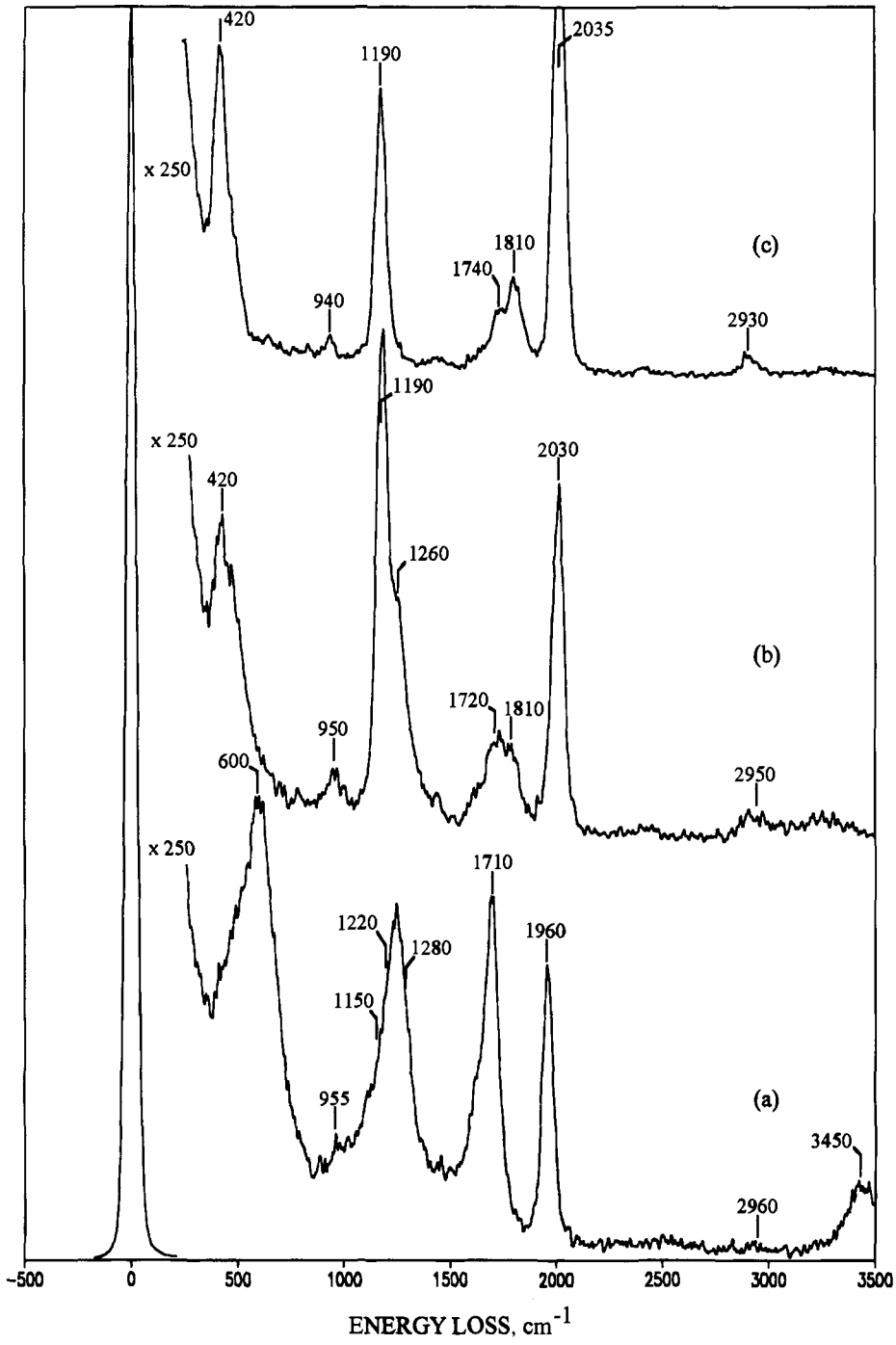

Figure 7. HREEL spectra recorded after exposure of a saturated overlayer of CO on Ru(001) to approximately 20 L of atomic hydrogen at 100 K, followed by annealing to (a) 150 K, (b) 180 K, and (c) 220 K.

5 L, and contains a carbon-oxygen bond, the order of which is between one and two (since ν(CO) is approximately 1280 cm^{-1}). This suggests the presence of η^2(C,O)-H_2CO. Moreover, there is ample precedent in the organometallic literature for formaldehyde bonded in an η^2-coordination with CO stretching frequencies between 1017 and 1220 cm^{-1}.[47] This species has also been isolated previously on Ru(001) by adsorbing formaldehyde from the gas phase,[10,p] but with a much lower CO stretching frequency of 1000 cm^{-1}. The probable reason for this difference lies in the significantly lower coverages of η^2-formyl, η^2-formaldehyde, and CO (approximately 0.03, 0.10, and 0.15, respectively) in the earlier study, implying less depletion of the local density of electronic states at the metal Fermi level. This, in turn, implies greater backdonation into the π^*-orbital of the adsorbed H_2CO, which results in a weaker CO bond. The carbon–hydrogen modes at 1005 and approximately 1280 cm^{-1} in Figures 6a and 7a are tentatively identified as the wagging modes, $\omega(CD_2)$ and $\omega(CH_2)$, of the η^2-formaldehyde, respectively. Comparison of these mode assignments with the literature data is presented in Table 3.

As in the case of the 5 L exposure, the η^1-formyl almost completely decomposes to adsorbed CO and desorbing hydrogen, as well as converting to η^2-formyl, after annealing to 180 K for 60 s, cf., Figures 6b and 7b. In the hydrogen spectrum of Figure 7b, the peak due to η^2-H_2CO is now clearly resolved at 1260 cm^{-1} (overlapping CO stretch and CH_2 wag). The peak identifying the overlapping CO stretch and CH bend of η^2-HCO is apparent at 1190 cm^{-1} and has significantly increased in intensity. The CO stretch at 950 cm^{-1}, assigned earlier to a second form of η^2-formyl that results from the conversion of

Table 1. Mode Assignments[d] for η^1-Formyl Produced by CO Hydrogenation on Ru(001) with Corresponding Assignments for the Organometallic Model Compounds Rh(OEP)(HCO),[a] $V(cp_2)CO(HCO)$,[b] and $CH_3O(HCO)$[c]

vibrational mode	η^1-HCO				η^1-DCO	
	this work	ref 45a	ref 45b	ref 43	this work	ref 43
ν(CO)	1740	1690	1700	1754	1735	1739
ν(CH)	2970			2943	2200	2216
CH bending	1140			1032	895	870
				1371		1048

[a] Reference 45a. [b] Reference 45b. [c] Reference 43. [d] All frequencies are in cm^{-1}.

Table 2. Mode Assignments[b] for η^2-Formyl Produced by CO Hydrogenation on Ru(001) with the Corresponding Assignments for η^2-Formyl Resulting from Formaldehyde Decomposition on Ru(001)[a]

vibrational mode	η^2-HCO		η^2-DCO	
	this work	ref 1p	this work	ref 1p
(CO)	1190	1180	1210	1160
(CH)	2970	2900	2200	
CH		1065		825
bending	1190	1400	940	980

[a] Reference 1p. [b] All frequencies are in cm^{-1}.

Table 3. Mode Assignments[e] for η^2-Formaldehyde Produced by CO Hydrogenation on Ru(001) with Corresponding Assignments for the Organometallic Model Compounds $Os(PPh_3)(CO)_2(H_2CO)$,[a] $Fe[(MeO)_3P]_2(CO)_2(H_2CO)$,[b] $V(cp_2)(H_2CO)$,[c] and for η^2-Formaldehyde Resulting from Formaldehyde Adsorption on Ru(001)

vibrational mode	η^2-D_2CO					η^2-D_2CO	
	this work	ref 47a	ref 47c	ref 47d	ref 1p	this work	ref 1p
ν(CO)	1280	1017	1220	1160	980	1280	1020
$\nu_a(CH_2)$					2970		2225
$\nu_b(CH_2)$							
$\delta(CH_2)$					1465		1190
$\varrho(CH_2)$					840		620
$\omega(CH_2)$	1280				1160	1005	865

[a] Reference 47a. [b] Reference 47c. [c] Reference 47d. [d] Reference 1p. [e] All frequencies are in cm^{-1}.

η^1-formyl, is also clear. All of the above is consistent with the deuterium spectrum in Figure 6b. The CO stretch and CD_2 wag of η^2-D_2CO are assigned to 1280 and 1005 cm^{-1}, respectively. The corresponding modes of η^2-DCO are found at 1220 (CO stretch) and 945 cm^{-1} (CD bend). As before, the presence of CO adsorbed in a bridge site is identified by the peak at 1810–1850 cm^{-1} in both Figures 6b and 7b.

In order to verify that the source of the 240 K peak in the D_2 TPD spectrum of Figure 3b is η^2-formaldehyde, the surface was annealed to 220 K for 30 s, cf., Figures 6c and 7c. Clearly, the features assigned to chemisorbed formaldehyde are missing. For example, in the hydrogen spectrum of Figure 7c, the peak at 1190 cm^{-1} is now very narrow, since the shoulder due to η^2-H_2CO at 1260 cm^{-1} has completely disappeared. Likewise, the deuterated species in Figure 6c exhibits a narrow feature at 945 cm^{-1} implying that the strong CD_2 wag of η^2-D_2CO at 1005 cm^{-1} is no longer present. The increase in intensity of both 'bridge' and 'on-top' CO suggests that the formaldehyde has undergone complete decomposition to adsorbed CO and desorbed hydrogen. Some decomposition of the η^2-formyl also occurs, as evidenced by the intensity decrease in the peaks at 945 and 1220 cm^{-1} and 1190 cm^{-1} in the deuterium and hydrogen spectra, respectively. After annealing to 250 K, the η^2-formyl decomposes completely to adsorbed CO and desorbing hydrogen.

To present a clearer picture of the effect of increasing atomic exposure, HREEL spectra recorded after exposing the saturated CO overlayer at 100 K to 5, 20, and 45 L of atomic deuterium are presented in Figure 8. A comparison of the intensity of the adsorbed CO stretch at 1960–2010 cm^{-1} with the loss features assigned to products, for example, the ν(CO) mode of η^1-formyl, clearly indicates that the conversion of CO to formyl and formaldehyde increases markedly with atomic deuterium exposure. The mode at 1005 cm^{-1}, assigned to the CD_2 wag of η^2-formaldehyde, clearly increases in intensity at the expense of the bending modes due to *both* η^1- and η^2-formyl (at 900 and 950 cm^{-1}), suggesting that η^2-formaldehyde may be formed from both of the formyl intermediates. Similar intensity behavior in the much weaker CO stretching mode of η^2-formaldehyde at 1280 cm^{-1}, although expected, is not so clear in the spectra.

IV. Discussion

The results presented here show that while coadsorbed hydrogen (from H_2) and CO do not react under UHV conditions, atomic hydrogen incident from the gas phase hydrogenates adsorbed CO on Ru(001) at surface temperatures as low as 100 K. If the reaction proceeds via LH kinetics at these temperatures, it must result from populating a highly unstable and reactive hydrogen state (by virtue of adsorbing *atomic* hydrogen)[48] that is at least 20 kcal/mol higher in energy than the low coverage reactant state of hydrogen in Figures 1 and 2. However, this reactive form of adsorbed hydrogen would have an unrealistically low binding energy of 45 kcal/mol (or less), an energy which, according to our knowledge, has no precedent in either the surface science or organometallic literature. Furthermore, after exposure of atomic hydrogen on a surface containing fractional deuterium and CO coverages of 1 and 0.15, respectively, the EEL spectra[41] identify hydrogenated products only, i.e., there was no evidence for deuteration. Any LH reaction from an adsorbed hydrogen state on this surface would contain a mixture of deuterated and hydrogenated products. Hence, we conclude that this reaction proceeds via an ER-type mechanism where the incident hydrogen atom does not chemisorb before reaction with the chemisorbed CO.

There are two possible channels by which this ER reaction could occur and produce the observed formyl and formaldehyde products. The first channel involves a indirect mechanism in which the hydrogen atom is trapped but does not accommodate to the surface temperature prior to reaction, i.e., the atom loses the normal component of its gas-phase momentum while maintaining some parallel momentum. A similar mechanism has been discussed theoretically by Harris and Kasemo[49] and observed experimentally during the dissociative chemisorption of oxygen on Al(111)[50] and CO oxidation on Pt(111).[51] The second channel follows a direct path where the hydrogen atom inserts into the adsorbed CO without either trapping at the surface or accommodating to the surface temperature. In both

(47) (a) Brown, K. L.; Clark, G. R.; Headford, C. E. L.; Marsden, K.; Roper, W. R. *J. Am. Chem. Soc.* **1979**, *101*, 503. (b) Headford, C. E. L.; Roper, W. R. *J. Organomet. Chem.* **1983**, *244*, C53. (c) Berke, H.; Bankhardt, W.; Huttner, G.; von Seyerl, J.; Zolsnai, L. *Chem. Ber.* **1981**, *114*, 2754. (d) Gambarotta, S.; Floriani, C.; Chiesi-Villa, A.; Guastini, C. *J. Am. Chem. Soc.* **1982**, *104*, 2019. (e) Gambarotta, S.; Floriani, C.; Chiesi-Villa, A.; Guastini, C. *Organometallics* **1986**, *5*, 2425.

(48) The possibility of a "reactive" LH reactant state of hydrogen and CO resulting from the large repulsive interactions that would exist between high coverages of coadsorbed hydrogen and CO is discounted by the observation of reaction with atomic hydrogen at low CO coverages.[10a,41]

(49) Harris, J.; Kasemo, B. *Surf. Sci.* **1981**, *105*, L281.

(50) Brune, H.; Wintterlin, J.; Behm, R. J.; Ertl, G. *Phys. Rev. Lett.* **1992**, *68*, 624.

(51) Matsushima, T. *Surf. Sci.* **1983**, *127*, 403.

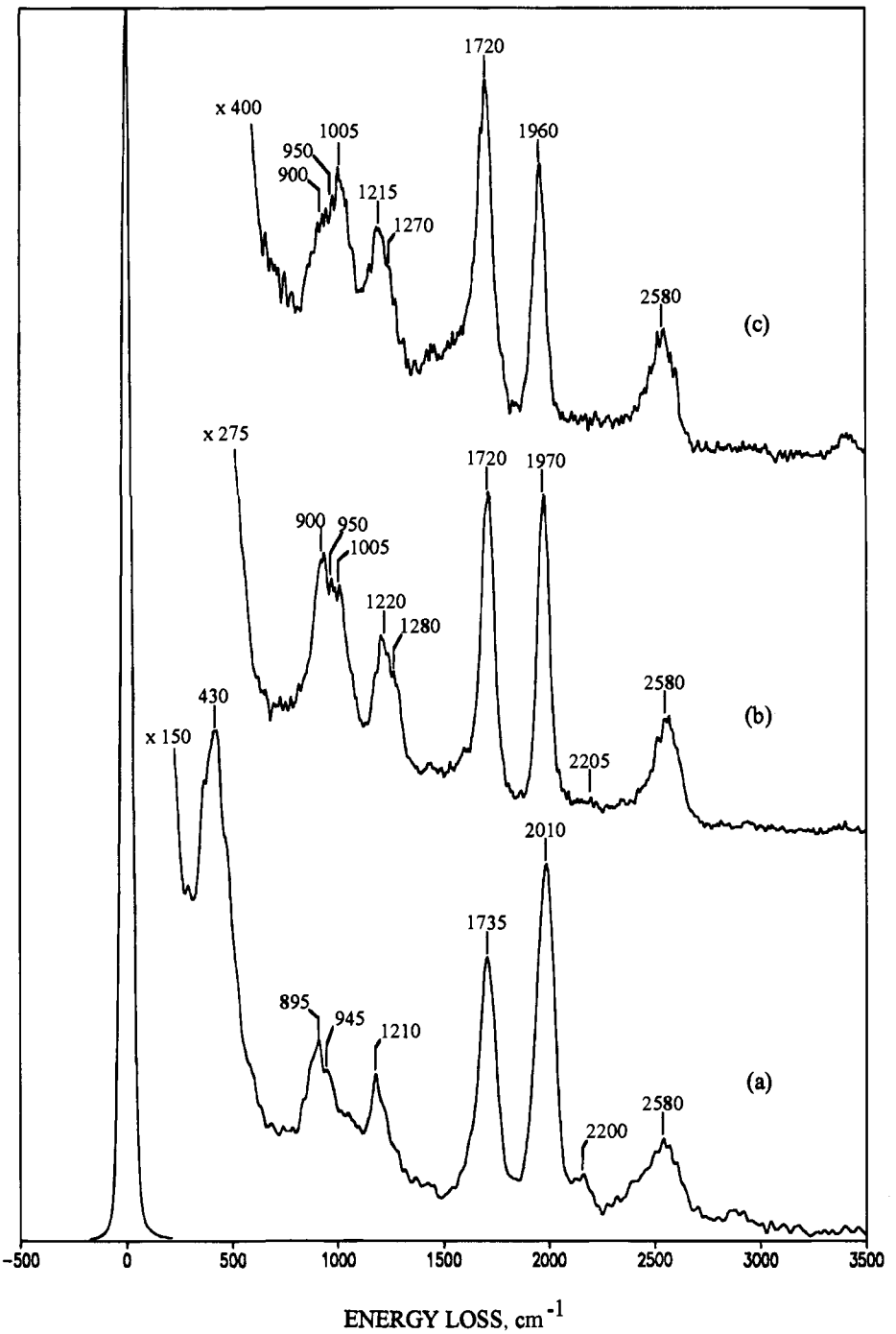

Figure 8. HREEL spectra recorded after approximate atomic deuterium exposures of (a) 5 L, (b) 20 L, and (c) 45 L on a saturated CO overlayer on the Ru(001) surface at 100 K, followed by annealing to 150 K.

cases, the hydrogen atom could react with either the oxygen atom of CO to form COH or with the carbon atom to produce formyl. We discount the COH reaction since there is no clear evidence for the presence of a stable, chemisorbed COH intermediate in the HREEL spectra. The possibility remains, however, that if COH did form, it could isomerize to HCO. Detailed *ab initio* calculations performed on the gas-phase H + CO system show this to be unlikely since the barrier to dissociation is less than half the barrier to isomerization from the metastable COH state.[52] These calculations also show that the direct formation of HCO is significantly favored (both thermodynamically and kinetically) over that of COH.

Irrespective of which dynamic channel occurs, the ER reaction is expected to proceed as follows. The hydrogen atom collides with an adsorbed CO molecule and an interaction of the 1s-orbital of hydrogen with the π^*-orbital of the CO rehybridizes the acyl carbon and leads to the formation of η^1-HCO, cf., Figure 9a. *Ab initio* studies of the formation of metalloformyl complexes (M−HCO) from organometallic hydridocarbonyls (H−M−CO), the prototypical carbonyl insertion reaction, demonstrate that the LH hydrogenation of CO would proceed first by hydride migration to the coadsorbed CO and then through a three-center transition state where the hydrogen 1s-orbital overlaps both a metal d_σ-orbital (bond scission) and a CO π^*-orbital (bond formation).[46,53] With this comparison in

(52) Geiger, L. C.; Shatz, G. C. *J. Phys. Chem.* **1984**, *88*, 214.

(53) (a) Berke, H.; Hoffmann, R.; *J. Am. Chem. Soc.* **1978**, *100*, 7224. (b) Ziegler, T.; Versluis, L.; Tschinke, V. *J. Am. Chem. Soc.* **1986**, *108*, 612. (c) Koga, N.; Morokuma, K. *J. Am. Chem. Soc.* **1986**, *108*, 6136. (d) Pacchioni, G.; Fantucci, P.; Koutecky, J.; Ponec, V. *J. Catal.* **1988**, *112*, 34 .

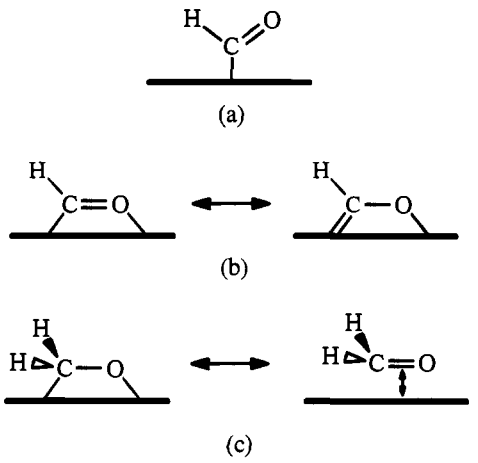

Figure 9. Proposed bonding structures for (a) η^1-formyl, (b) η^2-formyl, and (c) η^2-formaldehyde, as observed in both homogeneous and heterogeneous complexes.

mind, it would therefore be reasonable to expect that the initial intermediates resulting from the observed ER reaction to be essentially the same as those produced by the LH insertion reaction (observable only at higher temperatures and pressures),[54] since the two initiation steps closely resemble each other.

The η^2-formyl coordination results from overlap of the highest nonbonding orbital of the η^1-formyl (a lone pair on the oxygen atom) with empty metal d_σ-orbitals, along with backdonation from filled metal d_π-orbitals into the lowest unoccupied orbital of η^1-formyl (the π-orbital localized on the carbon atom) leading to a π-bond polarization (i.e., the π-bond is weakened so that the bonding electrons are localized on the more electronegative oxygen atom as a lone pair). This interaction has ample precedent in the organometallic literature[46b-d] where an η^2-formyl with a carbon-oxygen bond order between one and two has been identified, cf., the resonance structure given in Figure 9b. We expect the carbene structure (carbon-oxygen bond order of one) to be predominant for two reasons: (1) the CO stretching frequencies of the η^2-formyls are much lower than that of a CO double bond and (2) the dative lone pair bond from oxygen is weak, implying that the observed stability of the η^2-formyl is significantly dependent on the backdonation of charge from the metal into the π^*-orbital of the formyl.

The HREEL spectra (particularly those of Figure 8) seem to indicate that the formation of η^2-formaldehyde results from the interaction of the incident hydrogen atoms with both kinds of formyls. This interaction must involve the insertion of the hydrogen atom onto the formyl carbon atom at the expense of the carbon−metal σ bond. Consequently, the η^2-formaldehyde is bound to the metal via a dative bond from a lone pair on the oxygen atom to the metal along with the backdonation of charge from metal d_σ-orbitals into the π^*-orbital localized on the carbon atom.[55] Depending on the extent of overlap between the metal d_σ-orbitals and the π^*-orbital, either of the two bonding structures shown in Figure 9c can result. For a strong interaction, the CO bond order would be reduced to one and a "di-σ" bond to the metal would result, whereas for weaker interactions, the CO bond order falls only slightly below two and a "π" bond to the metal occurs, cf., Figure 9c. These configurations have been identified previously for the η^2-bonding of alkenes and acyls both on transition metal surfaces[56] and in homogeneous organometallic complexes.[46b-d,53] Based on our assigned frequency of the CO stretch at approximately 1280 cm^{-1}, we expect that the geometry of the η^2-formaldehyde observed here lies between these two extremes.

The mechanism of decomposition of the formyls and formaldehyde can be described as follows. By 200 K, η^1-formyl has both decomposed (to adsorbed CO and desorbed hydrogen) and converted to η^2-formyl. The η^2-formaldehyde, which forms at higher atomic exposures, almost exclusively decomposes to adsorbed CO and desorbed hydrogen by 240 K. No stabilization of the partial decomposition product, η^2-formyl, could be observed, because η^2-formyl has also begun to decompose at this temperature. Finally, the η^2-formyl is completely converted to adsorbed CO and desorbed hydrogen by 280 K.

V. Conclusions

The LH catalytic CO hydrogenation reaction that occurs under industrial conditions can proceed by two distinct routes, namely, a carbide mechanism involving the hydrogenation of surface carbon produced by the dissociative chemisorption of CO and a carbonyl insertion mechanism involving the insertion of hydrogen into molecularly adsorbed CO. We argue that (at least in the case of Ru) both mechanisms would be expected to make significant contributions to the overall production of hydrocarbons and oxygenates during this hydrogenation reaction. We have been able to probe the carbonyl insertion mechanism by effecting reaction between impinging gas-phase atomic hydrogen and adsorbed CO under UHV conditions (allowing HREEL spectroscopy to be used) and at surface temperatures as low as 100 K (permitting isolation of the reaction products). The atomic hydrogen overcomes both the thermodynamic and kinetic limitations which ordinarily restrict the FT synthesis to high pressures. As a result, we have been able to identify both η^1- and η^2-formyls as well as η^2-formaldehyde, which lends support to their existence as reaction intermediates during FT synthesis. This work represents the first spectroscopic verification of a carbonyl insertion mechanism (albeit via ER kinetics) for the CO hydrogenation reaction on any transition metal surface.

Acknowledgment. Primary support of this research was provided by the National Science Foundation (Grant CHE-9300020). Additional support was also provided by the Donors of the Petroleum Research Fund, administered by the American Chemical Society (Grant 28189-ACS).

JA943370U

(54) It is still expected that the all the elementary reactions that occur during the FT synthesis (e.g., hydrogenation, dissociation, migration, and insertion) obey LH kinetics, regardless of the reaction channel, i.e., carbide or insertion.

(55) Approximately 90° rotation (about the CO bond axis) must occur to transform from the trigonal and "distorted" trigonal shapes of the η^1-formyl [Figure 9a] and η^2-formyl [Figure 9b] structures, respectively, to the "distorted" tetrahedral shape of the η^2-formaldehyde structure, cf., Figure 9c. This implies that backdonation to π^* now originates from metal d_σ-orbitals (rather than d_π-orbitals as in the η^2-formyl case).

(56) Chatt, J.; Duncanson, L. A. *J. Chem. Soc.* **1953**, 2939.